Advanced Composite Materials
Publication details, including instructions for authors and subscription information:
http://www.tandfonline.com/loi/tacm20

Evaluation by FEM of temperature-dependent damage behavior in quasi-isotropic carbon/epoxy laminates

Hyoung Soo Kim [a], Wen-Xue Wang [b] & Yoshihiro Takao [c]

[a] Department of Aeronautics and Astronautics, Graduate School of Engineering, Kyushu University, 6-10-1 Hakozaki, Higashi-ku, Fukuoka 812-8581, Japan

[b] Research Institute for Applied Mechanics, Kyushu University, 6-1 Kasuga-Koen, Kasuga-city, Fukuoka 816-8580, Japan

[c] Research Institute for Applied Mechanics, Kyushu University, 6-1 Kasuga-Koen, Kasuga-city, Fukuoka 816-8580, Japan

Version of record first published: 02 Apr 2012.

To cite this article: Hyoung Soo Kim, Wen-Xue Wang & Yoshihiro Takao (1999): Evaluation by FEM of temperature-dependent damage behavior in quasi-isotropic carbon/epoxy laminates, Advanced Composite Materials, 8:3, 247-257

To link to this article: http://dx.doi.org/10.1163/156855199X00245

Adv. Composite Mater., Vol. 8, No. 3, pp. 247–257 (1999)

Evaluation by FEM of temperature-dependent damage behavior in quasi-isotropic carbon/epoxy laminates

HYOUNG SOO KIM [1,*], WEN-XUE WANG [2] and YOSHIHIRO TAKAO [2]

[1] *Department of Aeronautics and Astronautics, Graduate School of Engineering, Kyushu University, 6-10-1 Hakozaki, Higashi-ku, Fukuoka 812-8581, Japan*

[2] *Research Institute for Applied Mechanics, Kyushu University, 6-1 Kasuga-Koen, Kasuga-city, Fukuoka 816-8580, Japan*

Received 7 July 1998; accepted 29 August 1998

Abstract—Tensile tests of quasi-isotropic $(0/45/-45/90)_S$ Carbon Fiber Reinforced Plastic (CFRP) laminate at low (−100°C), room (25°C), and high (150°C) temperatures showed that the transverse crack propagation and interlaminar delamination growth behavior are obviously affected by the temperature. In the present study, the three-dimensional finite element method (FEM) is applied to a quasi-isotropic CFRP laminate to investigate the interlaminar free edge stresses and ply stresses under combined thermal and mechanical loadings. The mechanical properties of a lamina (T800H/#3631) are obtained experimentally as a function of temperature and both the temperature-dependent mechanical properties and the idea of stress-free temperature are taken into account. Resulting stresses, including initial residual thermal ones due to the stress-free temperature, are used to discuss the above mentioned experimental results, which leads to the temperature-dependent critical properties for damages such as transverse crack and delamination.

Keywords: CFRP; quasi-isotropic laminate; finite element analysis; interlaminar stress; residual thermal stress; temperature-dependent property.

1. INTRODUCTION

Carbon Fiber Reinforced Plastics (CFRP) have been widely used in aerospace and other application fields because of their high specific modulus and high specific strength, and they are expected to be applied in a wide range of temperature environments. In general, CFRP laminates are used in the form of multidirectional laminates in order to meet various required material properties and the different fiber orientations of the laminate may yield damage with various combinations of transverse cracks and delaminations. Recently, various effects of the temperature

*To whom correspondence should be addressed. E-mail: hyoungso@riam.kyushu-u.ac.jp

on the microscopic damage were investigated experimentally by Kim *et al.* [1] for quasi-isotropic carbon/epoxy composite laminates at low (−100°C), room (25°C) and high (150°C) temperatures under tensile loading.

CFRP laminates cured at around 180°C, being much higher than operating temperature, are expected to have initial residual thermal stresses which are a result of the difference in axial and transverse elastic properties (thermal expansion coefficients) of materials with unidirectional fiber reinforcement in each ply or at the interface. Moreover, mechanical properties of a lamina may be affected by the temperature, to which the polymer matrix is quite sensitive. Therefore, in order to understand thoroughly the interlaminar free edge and the ply stress problems of composite laminates, the initial residual thermal stresses and temperature-dependent mechanical properties should be taken into account.

The effect of thermal residual stresses near the interface and the free edge region has been investigated by Pagano and Hahn [2, 3], Wang and Crossman [4], and Griffin and Roberts [5, 6] for epoxy-based composite laminates. Ogi *et al.* [7] studied the hygrothermal damage problem of laminates and used temperature- and moisture-dependent elastic properties in their analysis. An analytical method by Wang *et al.* [8] to predict the transverse cracking of CFRP laminates under thermal and mechanical loadings incorporated initial residual thermal stresses. A few FEM analyses took into account the initial residual thermal stresses [9, 10] and temperature-dependent mechanical properties [11, 12], too.

In the present paper, the three-dimensional FEM is applied to a $(0/45/-45/90)_s$ quasi-isotropic CFRP composite laminates to investigate the relationship between stresses and damage behaviors at various temperatures, where initial residual thermal stresses and temperature-dependent mechanical properties are considered. The FEM analysis yields the interlaminar free edge stresses and ply stresses under combined thermal and mechanical loadings and leads to several conclusions concerning the damage sustained at different temperatures.

2. EXPERIMENTAL

Toughened-type carbon/epoxy composites of T800H/#3631 (Toray) were tested in a controlled thermostatic chamber to obtain the mechanical properties as a function of temperature. Four types of specimens shown in Table 1 were used. Stacking sequence, related mechanical properties, and specimen sizes are shown from left to right. A strain gauge is attached transversely also to the edge and surface of the specimen for measurement of ν_{TT} and ν_{LT}, respectively. The details are shown in [13]. Tensile tests [1] procedure of quasi-isotropic carbon/epoxy composite laminates with $(0/45/-45/90)_s$ and T800H/#3631 (Toray) are mentioned briefly for the completeness of the paper. The coupon specimen was 200 mm long, 6 mm wide, and 1.14 mm thick and both edges of the specimen were polished to observe the damage. The fiber volume fraction was about 60%. Tapered glass/epoxy tabs were bonded at the ends of the specimen, which resulted in a

Table 1.
Specimen layups and dimensions for various mechanical properties

Fiber orientation, Mechanical property	Width (mm)	Thickness (mm)	Length (mm)
(0_8), $[E_L, \nu_{LT}]$	12.7	1.14	229
(90_{16}), $[E_T]$	25.4	2.3	229
(90_{32}), $[\nu_{TT}]$	25.4	4.7	229
$(+45_2/-45_2)_{2s}$, $[G_{LT}]$	25.4	2.3	229

specimen gauge length of 60 mm. A strain gauge was mounted at the center of the specimen surface to measure the strain. Tensile tests were performed at a constant cross-head speed (0.5 mm/min) under three temperature environments, i.e. low (−100°C), room (25°C), and high (150°C) temperatures. After each full unloading, the transverse crack was microscopically observed and its density was quantitatively measured as a function of load by using an optical microscope. The interlaminar delamination growth behavior was non-destructively examined by a scanning acoustic microscope (SAM, Olympus UH Pulse 100 model, 30 MHz).

3. STRESS ANALYSIS

Initial residual thermal stresses due to thermal change from the stress-free temperature of 165°C [14] to testing temperatures, i.e. −100°C, 25°C, and 150°C are first obtained. Then the laminate loaded with a uniform axial strain ε_0 is calculated. A finite element code ABAQUS [15] is applied to a $(0/45/-45/90)_s$ carbon/epoxy rectangular laminate. Figure 1 shows geometry and finite element modeling of the upper half of the composite laminate, where u, v, and w are displacements of x, y, and z direction, respectively. The length a and width b of the laminate are $320h$ and $48h$, respectively, where the ply thickness $h = 0.125$ mm (see Fig. 1a). Since the laminate is symmetric, only the upper half body is divided into 20×24×12 8-node and 24-degree-freedom solid hexahedral elements, as shown in Fig. 1b, where the length along the x-axis is equally divided into 20 columns, the one along the y-axis is divided into 24 unequal rows with finer meshes in the vicinity of free edges and the thickness along the z-axis is equally divided into 4 layers which are again unequally divided into 3 layers. This model contains a total of 5760 solid elements and 6825 nodes. The following boundary conditions are chosen. For the initial residual thermal stress problem, w of all the nodes at $z = 0$, u, v, and w of node (0, 0, 0), u and v of node (0, 0, 0.5), and u of node (0, 6, 0) are set to be zero. For a uniform axial strain loading, in addition to the above mentioned boundary conditions, each u at a left-end is constrained and each u at a right-end is subjected to a uniform axial displacement of 0.4 mm corresponding to $\varepsilon_0 = 1\%$ in the x-direction.

4. RESULTS AND DISCUSSION

4.1. Mechanical properties of a lamina

The temperature-dependent mechanical properties obtained by experiment for the carbon/epoxy composite lamina (T800H/#3631) are listed in Table 2 together with the thermal expansion coefficients which are supposed to be defined as averages within the present temperature range.

4.2. Damage progresses [1]

Previous experimental results are also briefly summarized. Figure 2 shows stress-strain curves obtained from the tensile test at three temperatures of −100°C (low),

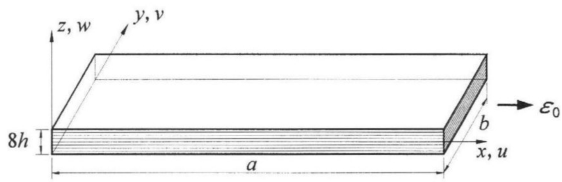

(a) Geometry of a $(0/45/-45/90)_S$ composite laminate
($a = 320h$, $b = 48h$, $h = 0.125$ mm)

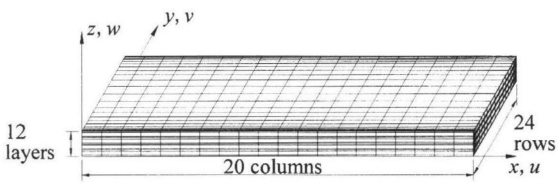

(b) Finite element modeling of the upper half of the $(0/45/-45/90)_S$ laminate

Figure 1. Geometry and finite element modeling of a $(0/45/-45/90)_S$ carbon/epoxy laminate subjected to a uniform axial strain $\varepsilon_0 = 1\%$.

Table 2.
Temperature-dependent mechanical properties of a carbon/epoxy (T800H/#3631) unidirectional lamina

T800H/#3631	Low temp.	Room temp.	High temp.
E_L (GPa)	156.5	154.6	139.7
E_T (GPa)	10.73	8.78	7.13
ν_{LT}	0.336	0.345	0.366
ν_{TT}	0.504	0.543	0.568
G_{LT} (GPa)	6.06	4.02	3.25
G^*_{TT} (GPa)	3.57	2.85	2.27
Thermal expansion coefficients [14]			
Longitudinal: $-0.6(\times 10^{-6}/°C)$		Transverse: $36(\times 10^{-6}/°C)$	

L and T denote the fiber and transverse direction, respectively.
$^*G_{TT}$ is calculated from $G_{TT} = E_T/2(1 + \nu_{TT})$.

25°C (room), and 150°C (high). Knee points at about 500 MPa to 540 MPa for −100°C and 25°C and 350 MPa to 400 MPa for 150°C are observed distinctly. It was found that this nonlinearity is caused by the large scale interlaminar delamination throughout the length of the specimen.

Figure 3 shows the edge damage state at room temperature (25°C). The transverse cracks are generated in both the 90° ply and −45° ply, and delaminations appear at 90/90, −45/90, and 45/−45 interfaces in this load. Most cracks in the −45° ply and delamination along the 90/90 and −45/90 interfaces start from the tips of 90° ply cracks, and free edge delamination at 45/−45 interface from the tips of −45° ply are observed.

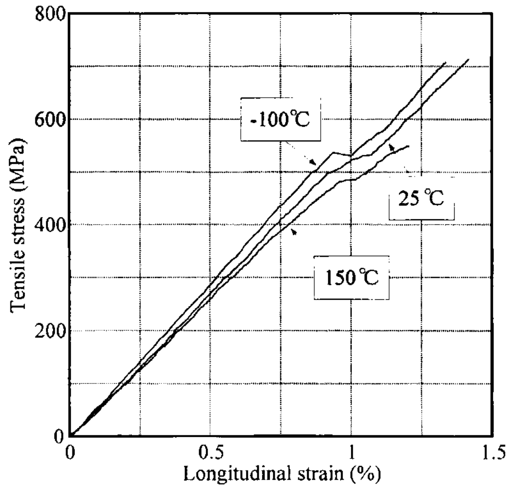

Figure 2. Stress–strain curves obtained from $(0/45/-45/90)_S$ carbon/epoxy laminate at various temperatures.

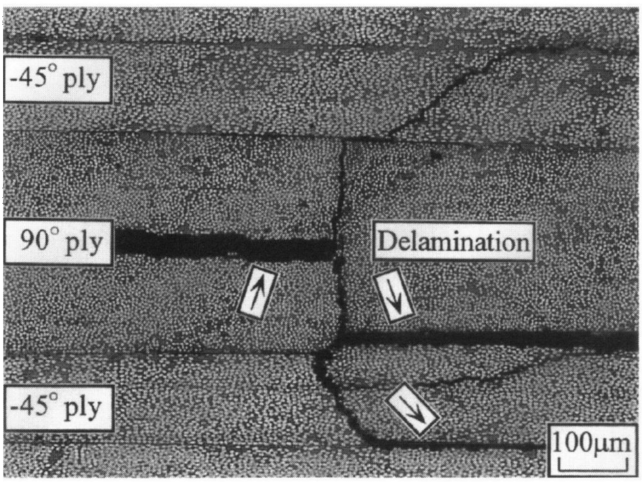

Figure 3. Damage state at free edge at room temperature (25°C, 560 MPa).

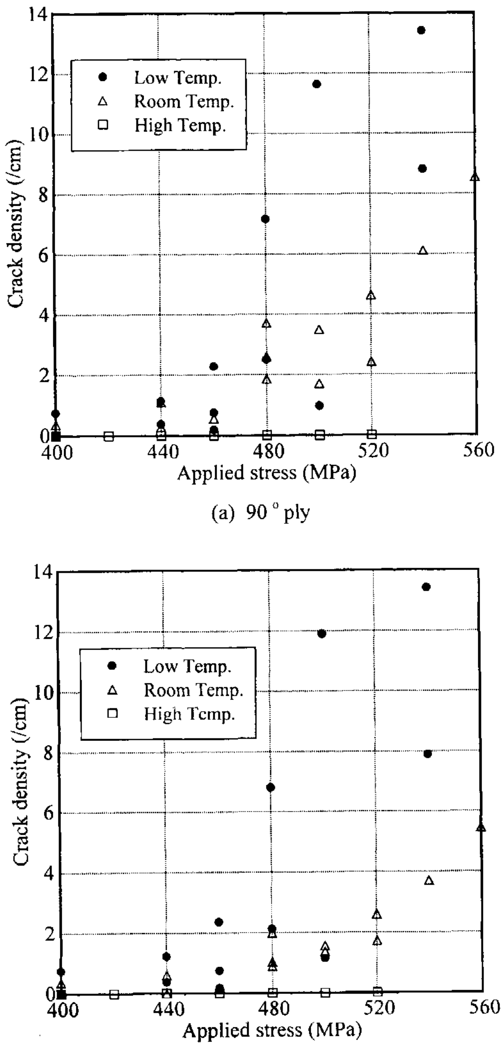

Figure 4. Crack density of a $(0/45/-45/90)_S$ carbon/epoxy laminate at various temperatures.

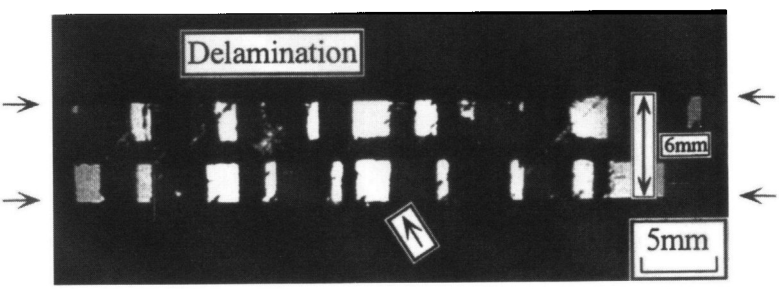

Figure 5. SAM image at −45/90 interface (25°C, 560 MPa: 30MHz) (→ ← : Free edge).

In Fig. 4, transverse crack densities in the 90° ply and the adjacent −45° ply are plotted for three temperatures. The crack density is defined as the number of cracks per centimeter. Crack density in both 90° and −45° ply increases when the temperature decreases. This might be due to the increase of initial residual thermal stresses.

Figure 5 shows delamination at the −45/90 interface observed by a scanning acoustic microscope (SAM, 30 MHz). The white area indicates the delaminated region. Figures 6a and 6b show the delamination area at 90/90 and −45/90 interfaces as a function of tensile stress.

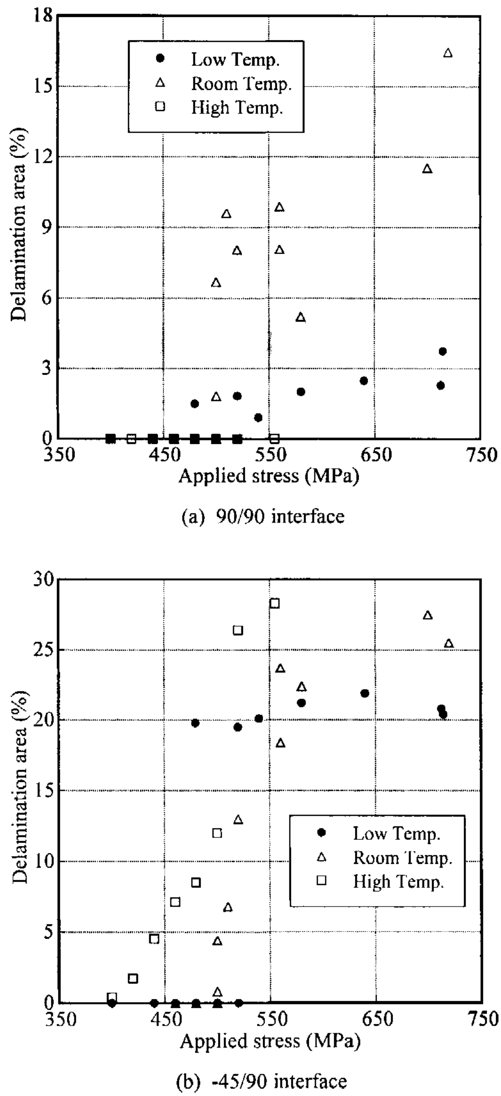

Figure 6. Delamination area of a $(0/45/-45/90)_S$ carbon/epoxy laminate at various temperatures.

In the case of the $-45/90$ interface, though the lower residual stress is expected, the delamination at a high temperature extends well. Thus, there might be the thermal degradation in the interlaminar fracture toughness. In the case of the 90/90 interface of Fig. 6a, it is found that the delamination area at room temperature is larger than that for the low and high temperature cases. The following characteristic damage at the high temperature should be mentioned: broken fibers with a through cut perpendicular to the fiber axis were observed in the 0° ply at the polished surface edge though they were neither before loading at the high temperature nor inside being more than 10 μm away from the polished surface edge. All broken fibers show their longitudinal cross-section on the surface edge due to polishing.

4.3. Stress distributions

The stress distributions along the y direction, including the initial residual thermal stress, are shown in Figs 7 and 8 for three temperatures, namely, -100°C, 25°C, and 150°C. Here, the center and free edge are denoted by 24 and 0 of $(b - y)/h$, respectively. Figure 7a shows the distributions of the normal stress σ_x at $x/a = 0.5$ in 0° ply. As shown in the figure, σ_x at a high temperature is lower than those at low and room temperatures, which means that the lower longitudinal Young's modulus ratio of a lamina at a high temperature, as shown in Table 2, decreases σ_x effectively in spite of the increase of σ_x arising from the thermal expansion mismatch, and is almost the same for various y. This σ_x does not explain that broken fibers are observed at the edge surface at a high temperature. Polished fibers might have some damage such as a small scratch due to wear or a kind of contact fatigue damage due to friction under contact stresses. It is assumed that this damage under a high temperature could lead to the effective low strength of fiber, though the complete fiber without any friction and wear does not show any temperature-dependent mechanical property within this temperature range [1].

The distributions of σ_x in the 90° ply and the normal stress σ_2 being perpendicular to a fiber in -45° ply and within xz plane $x/a = 0.5$ are shown in Fig. 7b. The stress increase with the temperature decreasing due to increase of initial residual thermal stresses and σ_x in the 90° ply is larger than σ_2 in the -45° ply. This Figure explains well the experimental results that the crack density both in the 90° and in the -45° ply increases with the temperature decreasing and that the transverse crack in 90° ply appears earlier than in the -45° ply. Figure 8 shows the distributions of σ_z and τ_{yz} at $x/a = 0.5$ for 90/90 and $-45/90$ interfaces. The τ_{xz} is omitted since its absolute value is quite small. The τ_{yz} is negligible compared to σ_z at the 90/90 interface and both have the same order at the $-45/90$ interface. Thus, it is reasonable to consider that the delaminaton at the 90/90 interface is caused by σ_z with the mode I fracture and that the one at the $-45/90$ interface is caused by both σ_z and τ_{yz} with the mixed mode fracture of I and II. Stresses in the vicinity of the free edge increase when the temperature decreases. This tendency does not agree with experimental results, that is, the delamination area is large for the room temperature at the 90/90 interface and for the high temperature at the

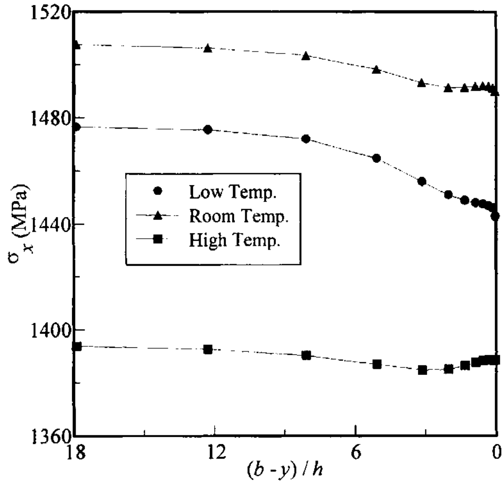

(a) 0 ° ply

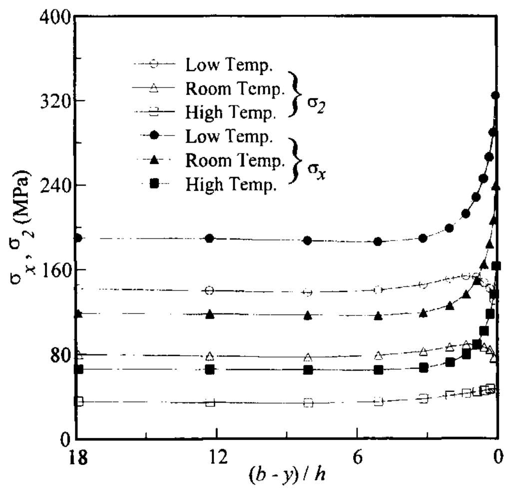

(b) σ_x in 90 ° ply and σ_2 in -45 ° ply

Figure 7. The distributions of stresses σ_x and σ_2 along y direction at $x/a = 0.5$ in each ply of the $(0/45/-45/90)_s$ carbon/epoxy laminate at various temperatures.

$-45/90$ interface. Since the delamination starts from the transverse crack tips, it might be necessary to perform the analysis with a crack together with obtaining the temperature-dependent critical strength of each damage mode.

5. CONCLUSIONS

The three-dimensional finite element method (FEM) is applied to a $(0/45/-45/90)_s$ quasi-isotropic CFRP composite laminates to investigate the relationship between

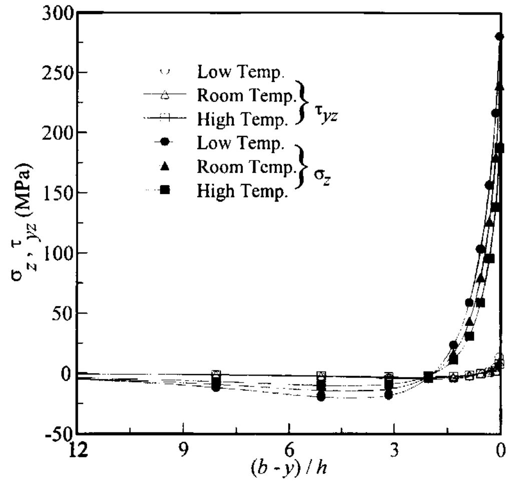

(a) 90/90 interface

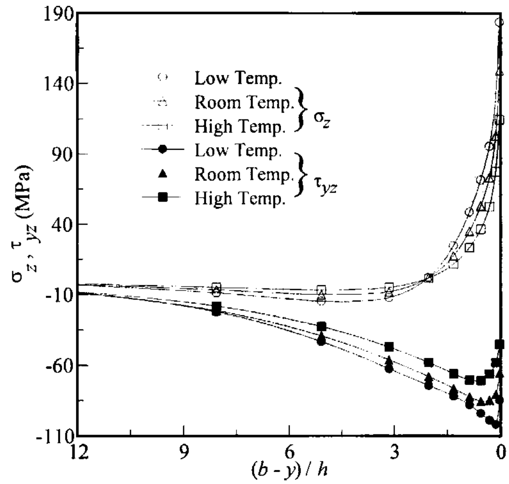

(b) -45/90 interface

Figure 8. The distributions of stresses σ_z and τ_{yz} along y direction at $x/a = 0.5$ at each interface of the $(0/45/-45/90)_S$ carbon/epoxy laminate at various temperatures.

stresses and damage behaviors at various temperatures, where initial residual thermal stresses and temperature-dependent mechanical properties are taken into account. The following conclusions are obtained.

(1) The fiber tensile strength at a polished edge surface might be affected by both friction and wear damage and temperature since the stresses at different temperatures could not explain the damage observed near the edge surface only at a high temperature.

(2) The transverse crack propagation both in the 90° and in the −45° ply is explained well by calculated stress distributions.

(3) The delaminations at the 90/90 and the −45/90 interfaces are predicted numerically to be the mode I and mixed mode of I and II, respectively.

(4) The delamination propagation behavior needs the research into the temperature-dependent strength of various interfaces.

REFERENCES

1. H. S. Kim, K. Ogi, T. Matsubara, W. X. Wang and Y. Takao, Microscopic damages of quasi-isotropic carbon/epoxy laminates at various temperatures, *J. Soc. Mater. Sci. Jpn.* **47**, 599–605 (1998) (in Japanese).
2. H. T. Hahn and N. J. Pagano, Curing stresses in composite laminates, *J. Compos. Mater.* **9**, 91–106 (1975).
3. N. J. Pagano and H. T. Hahn, Evaluation of composite curing stresses, in: *ASTM STP 617*, pp. 317–329. Am. Soc. for Testing and Mater. (1977).
4. A. S. D. Wang and F. W. Crossman, Edge effects on thermally induced stresses in composite laminates, *J. Compos. Mater.* **11**, 300–312 (1977).
5. O. H. Griffin, Jr. and J. C. Roberts, Numerical/experimental correlation of three-dimensional thermal stress distributions in graphite/epoxy laminates, *J. Compos. Mater* **17**, 539–548 (1983).
6. O. H. Griffin, Jr., Three-dimensional thermal stresses in angle-ply composite laminates, *J. Compos. Mater.* **22**, 53–69 (1988).
7. K. Ogi, H. S. Kim, T. Maruyama and Y. Takao, Influence of hygrothermal conditions on the damage processes in quasi-isotropic carbon/epoxy laminates, *Compos. Sci. Technol.* (in press).
8. W. X. Wang, H. S. Kim and Y. Takao, Evaluation of matrix cracking in the arbitrary layers of symmetric FRP laminates, in: *The 27th FRP Symposium Soc. Mater. Sci. Jpn.*, pp. 333–336 (1998) (in Japanese).
9. C. M. L. Wu, Nonlinear thermal and mechanical analysis of edge effects in angle-ply laminates, *Computers and Structures* **35**, 705–717 (1990).
10. C. M. L. Wu, Thermal and mechanical fatigue analysis of CFRP laminates, *Composite Structures* **25**, 339–344 (1993).
11. O. H. Griffin, Jr., Three-dimensional curing stresses in symmetric cross-ply laminates with temperature-dependent properties, *J. Compos. Mater.* **17**, 449–463 (1983).
12. J. K. Chen, C. T. Sun, and C. I. Chang, Failure analysis of a graphite/epoxy laminate subjected to combined thermal and mechanical loading, *J. Compos. Mater.* **19**, 408–423 (1985).
13. H. S. Kim, Microscopic damage of quasi-isotropic composite laminates under various temperatures, Kyushu University, Masters Thesis (1997) (in Japanese).
14. N. Takeda, H. Niizuma, S. Ogihara and A. Kobayashi, Experimental evaluation of thermal residual stress in CFRP cross-ply laminates, *Material System* **14**, 73–78 (1995) (in Japanese).
15. *ABAQUS/Standard User's Manual*, Version 5.6, Hibbitt, Karlsson and Sorensen, Pawtucket, RI, USA (1996).